Bootstrap Uncertainty Estimation of Canine Cardiac Fibers Anisotropy and Diffusivity on DT-MRI Data

T Pieciak

AGH University of Science and Technology, Krakow, Poland

Abstract

Diffusion tensor magnetic resonance imaging (DT-MRI) is an emerging technique, which permits one to probe the arrangement of fibrous tissues noninvasively on a microstructural level. Due to the anisotropy nature of water movements in cardiac muscle, one is able to extract local fiber orientations. However, inherent cardiac cycle and respiratory system, significantly affect cardiac diffusion tensor imaging (DTI) data. As a consequence, considerable distortion of the DTI data leads to ambiguity in the eigenvalues of the diffusion tensors calculation and measures of anisotropy and diffusivity quantification.

Our research focused on the investigation of estimation the uncertainty of anisotropy and diffusivity measures of the canine cardiac DTI data. The fractional anisotropy (FA) and mean diffusivity (MD) of the diffusion tensor images are considered depending on basal, mid-cavity, apical, and apex the American Heart Association (AHA) segments.

1. Introduction

Diffusion is a spontaneous molecular spreading phenomenon occuring in fluids (e.g., water). In cardiac muscle, diffusion takes the directional form which is called anisotropy [1]. Due to cardiac cycle, patient movements and eddy currents, diffusion-weighted (DW) MR images are characterized by poor quality. In result, DT-MRI data obtained by fitting process of tensor elements is ambiguous and lead to subsequent inaccurate representations of fiber tracts in tractography algorithms. Therefore, regularization procedures were proposed to enhace cardiac DT-MRI data [2], but these techniques do not answer the question: how does the data uncertain is?

This problem for the first time was mentioned in [3] and [4], where parametric and non-parametric statistical analysis were performed on DT-MRI data of the brain. Recently, many researches focused on uncertainties of DTI parameters [5] as well as uncertainty of tractography algorithms [6]. In [7] "cone of uncertainty" maps on synthetic data were proposed and in [8] were reinvestigated to in vivo data. This approach visualizes uncertainties of eigenvectors on a par with fiber tracts. A comprehensive comparison of bootstrap approaches for estimation of uncertainties of DTI parameters are found in [9].

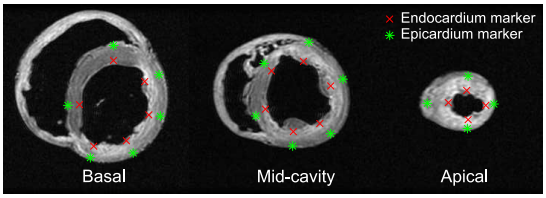

Figure 1. Bootstrap point's arrangement in basal, mid-cavity and apical planes (080803 data set).

The aim of this research is to investigate the uncertainty of anisotropy and diffusivity measures depending on the basal, mid-cavity, apical, and apex planes of the canine heart. To estimate probability density functions, a conventional bootstrap technique method was used. Then, the bootstrap estimates of standard errors were obtained on 17-segment AHA model and mapped onto cardiac polar maps (bull's eye diagrams).

2. Materials and methods

2.1. DWI cardiac data

The research was performed on six normal canine ex vivo hearts imaged by 1.5 T GE CV/I MRI Scanner with 40 mT/m maximum gradient strenght and 50 T/m/s slew rate. Each heart was placed in an acrylic container filled with Fomblin. The long axis of the hearts was aligned with the z-axis of the scanner. Then, the 3D Fast Spin Echo (FSE) protocol was used with uniformly distributed gradient directions between 16 and 28. Two images in each dataset are obtained with negligible small gradient. The temperature of the hearts varied between 18° C and 25° C.

Thirty-three points in single dataset (12 basal, 12 mid-cavity, 8 apical and one in apex plane) were chosen manually according to standard 17-segment model as a basis for the bootstrap procedure (fig. 1).

2.2. Anisotropy and diffusivity indices

So far, many geometrical indices of diffusion tensors were proposed including mean diffusivity (MD) and fractional anisotropy (FA) as well as Westin metrics [10]. However, predominantly only MD and FA are being widely used. Mean diffusivity is defined as follows:

$$MD = \frac{\lambda_1 + \lambda_2 + \lambda_3}{3} \tag{1}$$

and fractional anisotropy is given by:

$$FA = \sqrt{\frac{3}{2}} \frac{\sqrt{\sum_{i=1}^{3} (\lambda_i - MD)^2}}{\sqrt{\sum_{i=1}^{3} \lambda_i^2}} \tag{2}$$

where $\lambda_1, \lambda_2, \lambda_3$ are eigenvalues of the diffusion tensor.

2.3. The bootstrap resampling technique

The empirical non-parametric bootstrap technique has been used to obtain uncertaintly of MD and FA parameters according to AHA segment. The bootstrap technique provides us an estimate of the uncertainty of a given statistic based on multiple drawing from a pool of data [11]. In each stage of the procedure, i-th, a sample data of the same size is being drawn with replacement, called bootstrap sample. Then, an estimate $\widehat{\theta}_i^*$ of unknown statistic θ is being calculated. Repeating this scheme many times, one is able to obtain a probability density function (PDF), thus, a measure of uncertainty of a given statistic. Clearly, the bootstrap algorithm allows repetition an experiment in silico many times, as if it would be possible in practice. Unfortunately, reduplication of MRI scan hundreds times and even more of one patient is simply impossible.

2.4. The algorithm

The following four steps algorithm using a simple marker pointed out manually has been applied (fig. 1):
1. Create a pool of data $S = \{S_1, \ldots, S_5\}$ by acquiring DW signals from four neighbouring points (up, down, left, right), plus additional DW signal from initial point indicated manually. Hence, pool of data of size $5 \times n_G$ is obtained, where n_G denotes a DW gradient directions amount plus one value with negligible small gradient.
2. Draw with replacement, from the pool of data, S, a bootstrap sample S_i^* of size $1 \times n_G$. Each element of S_i^*, related to k-th direction ($k = 1, \ldots, n_G$), is chosen randomly among corresponding directions of S.
3. A second-order tensor, $\mathbf{D}$, is being fitted using a multivariate linear regression solved by nonnegative least-squares constraints problem [12]. For that reason, diffusion tensor eigenvalues are equal or greather then zero.
4. Calculate the estimates of $\widehat{MD}_i^*$ and $\widehat{FA}_i^*$, according to equations (1) and (2), based on the fitted diffusion tensor, $\mathbf{D}$.

Afterwards, steps 2-4 are being repeated multiple times (e.g., $n = 1000$).

Last but not least, the bootstrap standard errors of MD and FA parameters of endo- and epicardium were counted. The bootstrap estimate of standard error $\widehat{se}_B$ of a given statistic $\widehat{\theta}$ is defined as [11]:

$$\widehat{se}_B = \sqrt{\frac{1}{n-1} \sum_{i=1}^{n} \left(\widehat{\theta}_i^* - \widehat{\theta}_\bullet^*\right)^2} \tag{3}$$

where $\widehat{\theta}_\bullet^*$ is given by:

$$\widehat{\theta}_\bullet^* = \frac{1}{n} \sum_{i=1}^{n} \widehat{\theta}_i^* \tag{4}$$

3. Results

Probability density functions of FA and MD parameters were obtained according to basal, mid-cavity and apical planes, both endo- and epicardium regions (fig. 2). Either double or triple peaks in shape of MD's distributions are related to local variability of the tissue around markers. Notably, tissue variability is bound up with cardiac motion and systematic errors that are introduced to diffusion tensors, which in fact, are very difficult to describe in a parametric way. Bootstrap standard errors of MD are the lowest at inferior segments as well as basal plane (excluding inferolateral endocardium segment) (fig. 3).

All shapes of FA's PDFs at first glance, look like as normal distributions, but few of them do not qualify Lilliefors test for normality at null hypothesis at the 5% significance level. On the contrary to MD, bootstrap standard errors of FA are tending downwards in apical plane (fig. 3).

In table 1 expected values and standard deviations of MD and FA parameters are embedded based on 080803 data set.

4. Conclusions and remarks

In this paper, a bootstrap technique has been employed in DT-MRI data to calculate probability density functions of MD and FA parameters for endo- and epicardium on 17-segment AHA model. Hence, measures of uncertainties of mean diffusivity and fractional anisotropy as well as their bootstrap standard errors over cardiac muscle have been obtained and subsequently mapped onto cardiac polar maps.

A major weakness of the proposed method is drawing from diffusion-weighted signals of neighbourhood points, called *ROI bootstrap* by [4], instead of the diffusion-weighted signals coming from MRI scan repetitions.

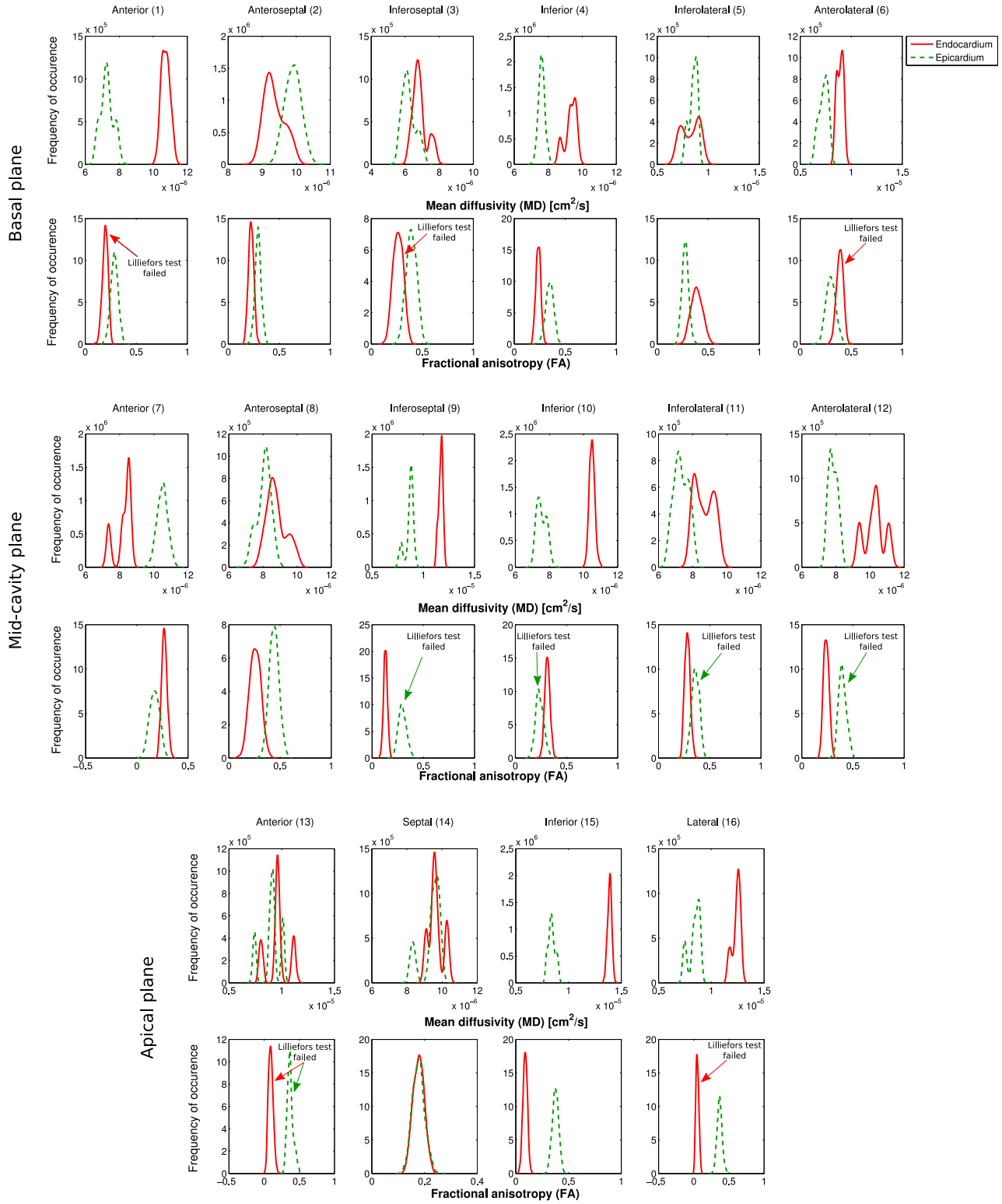

Figure 2. Probability density functions of mean diffusivity (odd rows) and fractional anisotropy (even rows) of basal, mid-cavity and apical AHA segments. Red and green colours were attributed to endo- and epicardium markers, respectively as shown in fig. 1. Numbers in brackets refer to AHA segment. Furthermore, null hypothesis rejection of Lilliefors normality test were marked on FA's probability density functions. (080803 data set).

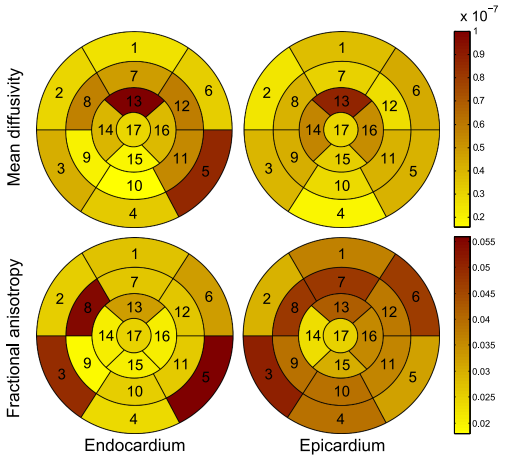

Figure 3. Distribution of bootstrap standard error $\widehat{se}_B$ of mean diffusivity (top) and fractional anisotropy (bottom) according to AHA region (080803 data set).

Table 1. The diversity of expected values and standard deviations of MD and FA indices (i-th row refers to i-th AHA segment). Specified standard deviations correspond to regions with the highest bootstrap standard error (fig. 3).

Mean diffusivity ($\times 10^{-6}$)		Fractional anisotropy	
Endo-	Epi-	Endo-	Epi-
10.7 ± 0.26	7.28 ± 0.38	0.20 ± 0.03	0.29 ± 0.04
9.35 ± 0.30	9.90 ± 0.24	0.22 ± 0.03	0.29 ± 0.03
6.85 ± 0.43	6.21 ± 0.40	$0.26 \pm \mathbf{0.05}$	$0.39 \pm \mathbf{0.05}$
9.31 ± 0.34	7.61 ± 0.19	0.24 ± 0.02	0.35 ± 0.04
$8.25 \pm \mathbf{0.86}$	8.54 ± 0.41	$0.39 \pm \mathbf{0.06}$	0.28 ± 0.03
8.91 ± 0.32	7.29 ± 0.45	0.39 ± 0.03	$0.30 \pm \mathbf{0.05}$
8.20 ± 0.48	10.5 ± 0.31	0.27 ± 0.03	$0.17 \pm \mathbf{0.05}$
8.78 ± 0.58	8.06 ± 0.42	$0.26 \pm \mathbf{0.05}$	$0.44 \pm \mathbf{0.05}$
11.7 ± 0.21	8.64 ± 0.43	0.13 ± 0.02	0.30 ± 0.04
10.5 ± 0.16	7.54 ± 0.28	0.31 ± 0.03	0.24 ± 0.04
8.66 ± 0.55	7.33 ± 0.42	0.28 ± 0.03	0.36 ± 0.04
10.3 ± 0.59	7.83 ± 0.27	0.24 ± 0.03	0.40 ± 0.04
$9.62 \pm \mathbf{1.01}$	$9.00 \pm \mathbf{0.88}$	0.09 ± 0.03	0.37 ± 0.04
9.65 ± 0.41	9.38 ± 0.56	0.18 ± 0.02	0.18 ± 0.02
13.9 ± 0.20	8.41 ± 0.33	0.09 ± 0.02	0.38 ± 0.03
12.4 ± 0.39	8.37 ± 0.54	0.05 ± 0.02	0.37 ± 0.04
8.64 ± 0.30		0.30 ± 0.02	

This assumption has been made, since we do not possess multiple scans of the heart.

In future investigations, either residual or wild bootstrap approach, which were introduced to DT-MRI in [5, 6, 9] for brain data analysis, should be considered. These bootstrap principle modifications allow to quantify uncertainties even though only one scan per direction is available. Moreover, one could acquire multiple heart scans and compare to Monte Carlo simulations of the DT-MRI experiment.

However, earlier, one should answer a fundamental question: does the uncertainty of DT-MRI cardiac data need to be measured in view of cardiac motion?

Acknowledgements

We are thankful to Drs. Patrick A. Helm and Raimond L. Winslow at the Center for Cardiovascular Bioinformatics and Modeling and Dr. Elliot McVeigh at the National Institute of Health for provision of data.

References

[1] Sosnovik DE, Wang R, Dai G, Reesee TG, Wedeen VJ. Diffusion MR tractography of the heart. J Cardiov Magn Reson 2009;11:47.

[2] Frindel C, Croisille P, Zhu YM. Comparison of regularization methods for human cardiac diffusion tensor MRI. Med Image Anal 2009;13:405–18.

[3] Pajevic S, Basser PJ. Non-parametric statistical analysis of diffusion tensor MRI data using the bootstrap method. 7th Annual Meeting ISMRM 1999;1790

[4] Pajevic S, Basser PJ. Parametric and non-parametric statistical analysis of DT-MRI data. J Magn Reson 2003;161:1–14

[5] Whitcher B, Tuch DS, Wang L. The wild bootstrap to quantify variability in diffusion tensor MRI. Proc Intl Soc Mag Reson Med 2005;13:1333

[6] Jones DK. Tractography Gone Wild: Probabilistic Fibre Tracking Using Wild Bootstrap With Diffusion Tensor MRI. IEEE Trans Med Imag 2008;27:1268–73.

[7] Basser PJ. Quantifying errors in fibre-tract direction and diffusion tensor field maps resulting from MR noise. 5th Annual Meeting ISMRM 1997;1790

[8] Jones DK. Determining and Visualizing Uncertainty in Estimates of Fiber Orientation from Diffusion Tensor MRI. Magn Reson Imag 2003;49:7–12.

[9] Chung SW, Lu Y, Henry RG. Comparison of bootstrap approaches for estimation of uncertainties of DTI parameters. NeuroImage. 2006;33:531–41.

[10] Westin CF, Maier SE, Mamata H, Nabavi A, Jolesz FA, Kikinis R. Processing and visualization for diffusion tensor MRI. Med Image Anal 2002;6:93–108

[11] Efron B, Tibshirani RJ. An Introduction to the Bootstrap. Chapman and Hall/CRC 1994

[12] Lawson CL, Hanson RJ. Solving Least Squares Problems. SIAM 1987

Address for correspondence:

Tomasz Pieciak
AGH University of Science and Technology
Al. Mickiewicza 30
30-059 Krakow
pieciak@agh.edu.pl